Published in final edited form as:
Invest Ophthalmol Vis Sci. 2009 February ; 50(2): 691–701. doi:10.1167/iovs.08-2136.

Performance of Confocal Scanning Laser Tomograph Topographic Change Analysis (TCA) for Assessing Glaucomatous Progression

Christopher Bowd[1], **Madhusudhanan Balasubramanian**[1], **Robert N. Weinreb**[1], **Gianmarco Vizzeri**[1], **Luciana M. Alencar**[1], **Neil O'Leary**[2], **Pamela A. Sample**[1], and **Linda M. Zangwill**[1]

[1] Hamilton Glaucoma Center and the Department of Ophthalmology, University of California, San Diego, La Jolla, California

[2] Department of Optometry and Visual Science, City University, London, United Kingdom

Abstract

Purpose—To determine the sensitivity and specificity of confocal scanning laser ophthalmoscope's Topographic Change Analysis (TCA; Heidelberg Retina Tomograph [HRT]; Heidelberg Engineering, Heidelberg, Germany) parameters for discriminating between progressing glaucomatous and stable healthy eyes.

Methods—The 0.90, 0.95, and 0.99 specificity cutoffs for various (n = 70) TCA parameters were developed by using 1000 permuted topographic series derived from HRT images of 18 healthy eyes from Moorfields Eye Hospital, imaged at least four times. The cutoffs were then applied to topographic series from 36 eyes with known glaucomatous progression (by optic disc stereophotograph assessment and/or standard automated perimetry guided progression analysis, [GPA]) and 21 healthy eyes from the University of California, San Diego (UCSD) Diagnostic Innovations in Glaucoma Study (DIGS), all imaged at least four times, to determine TCA sensitivity and specificity. Cutoffs also were applied to 210 DIGS patients' eyes imaged at least four times with no evidence of progression (nonprogressed) by stereophotography or GPA.

Results—The TCA parameter providing the best sensitivity/specificity tradeoff using the 0.90, 0.95, and 0.99 cutoffs was the largest clustered superpixel area within the optic disc margin ($CAREA^{disc}$ mm^2). Sensitivities/specificities for classifying progressing (by stereophotography and/or GPA) and healthy eyes were 0.778/0.809, 0.639/0.857, and 0.611/1.00, respectively. In nonprogressing eyes, specificities were 0.464, 0.570, and 0.647 (i.e., lower than in the healthy eyes). In addition, TCA parameter measurements of nonprogressing eyes were similar to those of progressing eyes.

Conclusions—TCA parameters can discriminate between progressing and longitudinally observed healthy eyes. Low specificity in apparently nonprogressing patients' eyes suggests early progression detection using TCA.

Confocal scanning laser ophthalmoscopy (CSLO) is a proven technique for identifying eyes with glaucomatous optic disc damage.[1,2] This is a difficult task complicated by the very large range in the number of ganglion cell axons (represented by neuroretinal rim volume at the optic

Corresponding author: Christopher Bowd, Hamilton Glaucoma Center, 178, Department of Ophthalmology, University of California, San Diego, La Jolla, CA, 92037-0946; cbowd@eyecenter.ucsd.edu.

Disclosure: **C. Bowd**, Lace Elettronica (F); **M. Balasubramanian**, Heidelberg Engineering (F); **R.N. Weinreb**, Carl Zeiss Meditec (F, C), Heidelberg Engineering (F); **G. Vizzeri**, None; **L.M. Alencar**, None; **N. O'Leary**, None; **P.A. Sample**, Carl Zeiss Meditec (F), Haag-Streit (F), Welch-Allyn (F); **L.M. Zangwill**, Carl Zeiss Meditec (F), Heidelberg Engineering (F), Optovue (F)

disc) in healthy eyes.[3,4] This extensive range results in considerable overlap in CSLO-based optic disc topography measurements between healthy and glaucomatous eyes. A potentially less complicated task is the detection of change (e.g., disease-related progression) in optic disc topography over time in individual eyes. However, relatively few studies have been undertaken to assess the ability of CSLO to accomplish this task (e.g., Refs. 5–14).

The primary method for assessing glaucomatous change using CSLO is Topographic Change Analysis (TCA) with the Heidelberg Retina Tomograph (HRT; Heidelberg Engineering, Heidelberg, Germany), a technique that compares the variability within a baseline examination to that between baseline and follow-up examinations. By using a nested three-way ANOVA model that accounts for the effects of topograph scan variability, scan time (i.e., baseline or follow-up), and location of topograph height measurements as model factors, TCA describes significant, repeatable change on the superpixel (4 × 4 pixels) level.[6,15] Briefly, an array of probabilities, indicating the probability of change at each superpixel is created, and contiguous superpixels showing significant decreases in retinal height ($P < 0.05$ with changes repeatable across multiple examinations required) are clustered, thus allowing the creation of various TCA change summary parameters describing size and location of regions of change. As an example, one parameter that can be examined is the number of superpixels in the largest observed cluster of changed locations. Although this technique identifies *superpixel-wise* or *cluster-wise* significant change, there currently are few suggestions as to what defines a *clinically* significant change in a follow-up examination. Identifying descriptors of clinically significant change is complicated by the fact that there is no true reference-standard for such change.

We used CSLO data sets obtained from the University of California, San Diego Hamilton Glaucoma Center and the Moor-fields Eye Hospital Glaucoma Research Unit, in an attempt to identify various TCA parameters to quantify progressive glaucomatous changes and to estimate corresponding parameter cutoffs that result in both a high sensitivity for identifying known progression, defined using currently accepted progression detection techniques (optic disc photograph assessment, and standard automated perimetry automated progression analysis), and a high specificity for identifying no progression in healthy eyes observed over time. Parameters and cutoffs with these characteristics may be good candidates for identifying clinically relevant progression. The performance of these parameters/cutoffs also was investigated in a large group of patients' eyes that were apparently stable, defined with current techniques. We hypothesized that TCA parameters with good sensitivity and specificity (as described above) would identify a significant proportion of "stable" patients' eyes as progressing, thus suggesting the possibility of early progression detection using CSLO TCA.

Methods

Subjects

Two hundred sixty-seven eyes of 202 participants enrolled in the UCSD Diagnostic Innovations in Glaucoma Study (DIGS) were included in the study. This number included all eyes examined (with good-quality images) with Heidelberg Retina Tomograph (HRTII; Heidelberg Engineering) at least four times and tested (with reliable results) with standard automated perimetry (SAP SITA standard and full threshold, Humphrey HFAII; Carl Zeiss Meditec, Dublin, CA) at least five times. In addition, eyes had to have stereophotography (TRC-SS; Topcon Instruments Corp. of America, Paramus, NJ) of the optic disc and SAP testing within 6 months of their first and most recent HRT examination. Both HRT[1] and SAP[16] have been described in detail previously. For HRT, good-quality images were those with image SD < 50 μm, even image exposure, and good centering. Of the more than 1250 DIGS topographies used in this study, nine had SDs between 40 and 50 μm. The median SD for all DIGS topographies included was 15.0 (25% quartile, 12.0; 75% quartile, 20.0). For SAP, reliability was defined as false positives, fixation losses, and false negatives ≤ 25% with no

observable testing artifacts. All stereophotographs were considered to be of fair to excellent quality by trained observers.

In addition to the testing, each study participant underwent a comprehensive ophthalmic evaluation, including a review of medical history, best corrected visual acuity testing, slit lamp biomicroscopy, intraocular pressure (IOP) measurement with Goldmann applanation tonometry, gonioscopy, and dilated slit lamp fundus examination with a 78-D lens. To be included in the study, participants had to have a best corrected acuity better than or equal to 20/40, spherical refraction within ±5.0 D and cylinder correction within ±3.0 D, and open angles on gonioscopy. Eyes with coexisting retinal disease, uveitis, or non-glaucomatous optic neuropathy were excluded.

DIGS eyes were either healthy (n = 21 eyes with no history of IOP > 22 mm Hg, *and* healthy appearing optic disc by stereophotography, *and* SAP results within normal limits), had suspected glaucoma (n = 192 eyes with glaucomatous-appearing optic disc by stereophotograph assessment or examination, *or* repeatable SAP results outside normal limits, *or* ocular hypertension with healthy-appearing optic disc and SAP results within normal limits), *or* had glaucoma (n = 54 eyes with glaucomatous-appearing optic disc by stereophotograph assessment *and* repeatable SAP result outside normal limits) at the baseline imaging date. Glaucomatous-appearing optic discs were those with cup-to-disc area, rim thinning, *or* retinal nerve fiber layer (RNFL) defects indicative of glaucoma. SAP results outside normal limits were those with pattern standard deviation (PSD) with $P \leq 5\%$ *and*/*or* Glaucoma Hemifield Test results outside normal limits (StatPac analysis; Carl Zeiss Meditec). Ocular hypertension was defined as IOP > 22 mm Hg on at least two occasions.

CSLO images from 18 healthy eyes of 18 individuals imaged at the Glaucoma Research Unit of the Moorfields Eye Hospital (MEH), London, also were included in the study (see Selecting Specificity Cutoffs for TCA Parameters section for details; also Refs. 5,[7,11,13]).

All study methods adhered to the provisions of the Declaration of Helsinki for research involving human participants and the Health Insurance Portability and Accountability Act (HIPAA), when applicable.

Classification of Eyes

Each patient's eye was classified as *progressed* (n = 36) or *not progressed* (n = 210) over the course of this longitudinal study. Demographic characteristics at baseline of both groups are shown in Table 1. Progression was defined as *either* progressive change in the appearance of the optic disc on stereophotograph assessment *or* a result of "likely progression" based on SAP Guided Progression Analysis (GPA, software version 4.2). Progressive change in the photographic appearance of the optic disc was defined as an increase in neuroretinal rim thinning or RNFL defect size or the appearance of a new RNFL defect. Evidence of progression was based on masked (patient name, diagnosis, and temporal order of photographs) comparison between the baseline and most recent photograph, by two observers. If these observers disagreed, a third observer served as an adjudicator. The temporal order of each progression pair was unmasked after final assessment. Overall agreement among observers in the evaluation of photographs of progressed and nonprogressed eyes was 0.922, with $\kappa = 0.566$ (95% confidence interval [CI], 0.387–0.745). Photographs of 6 of the 20 eyes that progressed by optic disc photographs required adjudication, and photographs of 12 of 210 of the nonprogressed eyes required adjudication. "Likely progression" by SAP GPA was defined as a significant decrease from baseline (two examinations) pattern deviation at three or more of the same test points on three consecutive tests (i.e., EMGT criterion[17]). Of the 36 progressed eyes, 15 eyes progressed by stereophotograph assessment alone, 16 eyes progressed by SAP GPA alone, and five eyes progressed by both techniques.

TCA Processing and Parameters Assessed

All the DIGS HRT examinations in the study were conducted with the same HRT-II instrument and the MEH examinations were conducted with HRT-I. The DIGS and MEH HRT data were imported into HRT 3 system software (ver. 3.1.2; Heidelberg Engineering) for topograph alignment and TCA. For quantitative analysis, TCA superpixel change probabilities of each follow-up examination and all topographies aligned with the baseline topograph of each eye were exported from the HRT 3 software (TCA change probability exports are available as .txt files, and the topographies are available as .raw files). All analysis was performed with commercial software (MatLab, ver. R2007a; The MathWorks, Natick, MA).

Using the change probability values and the superpixel mean difference image exported from the software, a change significance map was constructed for each follow-up examination by identifying the superpixel locations with significant decrease in the retinal height from the baseline examination (i.e., the locations with negative height change in the mean difference image and change probability < 0.05). Any significantly changed superpixel locations with fewer than four significantly changed superpixel neighbors were discarded. After filtering any isolated locations from the change significance maps, clinically significant TCA change locations were detected by identifying the superpixel locations with changes repeatable in two of the two, three of the three, or three of the four most recent follow-up examinations, depending on the number of follow-up examinations available at the time of evaluation (Heidelberg Engineering, personal communication, 2007).

Using the spatially filtered and clinically significant change maps, we computed 70 TCA parameters (Tables 2, 3, 4; Figs. 1, 2, 3). These parameters described the cluster of superpixels with the largest significant change in area (largest area superpixel cluster) or the largest significant change in volume (largest volume superpixel cluster), either within the optic disc margin (disc) or anywhere within the whole image field of view (total). We considered the number of superpixels within a cluster (*CSIZE*), area of a cluster (in square millimeters, *CAREA*), volume of a cluster (in cubic millimeters, *CVOL*), and cluster size in superpixels expressed as a percentage of optic disc area (*CSIZE%*). We also restricted these parameters to clusters in which each superpixel exhibited a height change from baseline of ≥0, ≥20, ≥50, ≥100, and ≥200 μm. The parameters investigated were similar to those previously suggested by Artes and Chauhan (Artes PH, et al. *IOVS* 2006;47:ARVO E-Abstract 4349).

From the possible follow-up examinations available for each eye, we chose the single follow-up examination with the largest repeatable change from baseline to describe the change in TCA results. This scheme was chosen out of several possible alternates—for example, the earliest or the latest follow-up examination showing repeatable change. Although this scheme was selective for the maximum change observed during the entire follow-up duration of an eye, it should not bias sensitivities and specificities, because all change was repeatable in at least two or three consecutive follow-up examinations or three of the four latest follow-up examinations (i.e., a parameter value estimated from a follow-up examination with the largest repeatable change is not an extreme outlier).

Selecting Specificity Cutoffs for TCA Parameters

We selected various specificity cutoffs for each TCA parameter by using the independent sample of longitudinal topographical series from healthy eyes obtained at MEH. MEH eyes were imaged on an average of 11.3 times (95% CI, 5.6–17.1) over an average follow-up of 5.8 years (95% CI, 3.1– 8.4) and were recruited based on the following criteria: IOP < 22 mm Hg on two or more occasions; two consecutive, reliable (<25% fixation losses; <30% false positives and false negatives) visual field examinations with an AGIS score of 0; no ocular disease; no family history of glaucoma or ocular hypertension; and age > 35 years (average

age, 74.2 years; 95% CI, 60.5–87.8). Images/series were well aligned and without apparent motion artifacts, magnification changes, image doubling or grainy appearance and baseline images were clear enough to visualize the scleral ring and therefore to accurately place a contour line. Of the 240 MEH topographies used in this study, 5 had an SD between 40 to 60 μm. The median SD for all MEH topographies included was 23.0 (25% quartile 17.0, 75% quartile 28.7).

Because desirable cutoffs could not be determined based on only 18 topographical series (e.g., less than two eyes would define the 0.90 specificity cutoff), we used a permutation technique to construct an acceptable number of series to derive 0.90, 0.95 and 0.99 specificity cutoffs for this population. This technique was based on the logic that if an eye is not progressing, differences between topographies should be solely attributable to unpredictable image variability (e.g., attributable to image quality, IOP differences). Because of this, the order of these follow-up topographies should be theoretically interchangeable. Based on this assumption, 1000 pseudolongitudinal series from the 18 MEH eyes were constructed. Each series was constructed by randomly rearranging of the order of the follow-up topographies of each single eye (the baseline examination was kept constant and only the order of the follow-up topographies was rearranged to ensure that the baseline condition of an observed longitudinal series was maintained in all the pseudolongitudinal series generated using it). All three HRT topographies that compose each follow-up mean examination were held together and rearranged as a whole (i.e., only the order of follow-up examinations was rearranged, not the order of the individual topographies). Each of these 18 eyes contributed approximately 56 pseudolongitudinal series for a total 1000 series (mean number of images used in each series was 11.3; 95% CI, 11.16–11.51). These 1000 permuted series allowed us to determine 0.90, 0.95, and 0.99 specificity cutoffs based on a reasonable number of longitudinal series (e.g., 50 series outside of normal limits to define 0.95 specificity). For each parameter, the largest repeatable (by HRT 3.0 requirement) TCA values from each series were pooled. Parameter cutoffs were estimated from the 90th, 95th, and 99th percentile of these pooled values.

Testing Sensitivity and Specificity of 0.90, 0.95, and 0.99 Parameter Cutoffs

The sensitivity of the newly developed cutoffs was tested in the group of 36 DIGS eyes that progressed based on optic disc and/or SAP testing. Specificity was tested on the group of 21 healthy eyes of 20 individuals, also enrolled in DIGS and meeting the study inclusion criteria. Healthy eyes were imaged an average of 4.1 times (95% CI, 3.5–4.7) over an average follow-up of 1.4 years (95% CI, 0.0–5.3) and were recruited based on the following criteria: IOP < 22 mm Hg on two or more occasions; reliable (<25% fixation losses, false positives, and false negatives) visual field examination results, with PSD and Glaucoma Hemifield Test within normal limits; healthy-appearing optic discs based on expert assessment of masked stereoscopic optic disc photographs; and no ocular disease. Average age was 63.6 years (95% CI, 31.9–95.2).

We also applied these cutoffs to the 210 patients' eyes determined to be stable by photograph assessment and SAP testing. Table 1 shows demographic, HRT follow-up details (years followed and number of follow-up examinations included in analyses) and baseline optic disc and visual field characteristics of progressed eyes and patient eyes stable by photography and SAP.

Previous evidence suggests poor agreement between progression detected based on optic disc assessment (e.g., by HRT, stereophotography) and progression detected based on visual field testing.[8,10,12] This poor agreement may confound our evaluation of TCA performance because both optic disc and SAP results were used as reference standards for progression. Because it may be more appropriate to describe TCA sensitivity in eyes progressing by optic disc

assessment alone, the sensitivity analyses were repeated on the 20 eyes that progressed by stereophotography, regardless of visual field progression.

Results

Table 2 shows sensitivities and specificities of the 0.99, 0.95, and 0.90 cutoffs (derived from the pseudolongitudinal series constructed from the 18 healthy MEH eyes) for all TCA parameters, based on the largest area superpixel cluster and largest volume superpixel cluster of significant decrease in retinal height, regardless of the retinal height change at each superpixel (i.e., retinal height change ≥ 0 μm and change probability < 0.05).

Sensitivity by disc and/or GPA describes the percentage of eyes with known progression by stereophotography and/or SAP GPA ($n = 36$) that were identified as progressed by TCA; *sensitivity by disc* describes the percentage of eyes with known progression by stereophotography ($n = 20$) that were identified as progressed by TCA; and *specificity* describes the percentage of healthy eyes followed up longitudinally that were identified as stable by TCA ($n = 21$). Table 3 and Figures 1 to 3 show results for the same parameters when the required height change from baseline for each superpixel was ≥ 20 μm (Table 3), ≥ 50 μm (Fig. 1), ≥ 100 μm (Fig. 2), and ≥ 200 μm (Fig. 3) with associated change probabilities < 0.05. In each table, the TCA cutoff that was used is presented after the sensitivity and specificity results. This information is also presented under each bar in the figures. Results for required superpixel height changes ≥ 50 μm are presented in the figures instead of the tables so that the reader can appreciate changes in sensitivity and specificity with changes in parameter cutoffs without being bogged down by too many numbers. Results from the largest volume superpixel clusters have been omitted from the figures because these results were nearly identical with results from the largest area superpixel clusters (described later).

In general, sensitivity was greatest when depth of defect was not considered, and specificity was greatest when a depth of defect ≥ 50 μm was required to identify a retinal location as significantly changed from baseline. In the former case, sensitivity (based on the disc and/or GPA criterion) ranged from 0.222 to 0.778 and specificity ranged from 0.809 to 1.00. In the latter case, ranges were 0.130 to 0.605 (sensitivity) and 0.952 to 1.00 (specificity). The parameter with the marginal best diagnostic accuracy (sensitivity/specificity tradeoff) overall was cluster area within the optic disc ($CAREA^{disc}$) with significantly changed pixels ≥ 0 μm, using the 0.90 specificity cutoff (sensitivity = 0.778, specificity = 0.809). Diagnostic accuracy was slightly better when measurements were obtained within the optic disc rather than across the entire field of view. In addition, diagnostic accuracy and parameter cutoffs for all depth-of-defect criteria were generally similar when comparing results from the largest area superpixel cluster to the largest volume superpixel cluster indicating that, in most cases, the area of retinal change and volume of retinal change criteria identified the same clusters. Finally, sensitivities were generally similar, regardless of the criterion used to define progression (by disc compared to by disc and/or GPA).

Figure 4 shows examples of agreement for detecting progression among TCA analysis, stereophotography assessment, and SAP GPA. Figure 4A shows an example of a true-positive TCA result. This eye progressed by stereophotograph assessment, SAP GPA, and TCA $CAREA^{disc}$ (using the 0.90 specificity cutoff of ≥ 0.036 mm^2). Inferior rim thinning was apparent in both the TCA image ($CAREA^{disc} = 0.252$ mm^2) and the stereophotograph pair. This change was reflected in significant superior hemifield change measured by GPA. Figure 4B shows an example of a false-negative TCA result. This eye progressed by stereophotograph assessment and SAP GPA, but not by TCA. Inferior rim thinning was apparent in the stereophotograph pair and was reflected in a significant superior hemifield change by GPA. However, the TCA image showed little clustered change ($CAREA^{disc} = 0.011$ mm^2). Finally,

Figure 4C shows a "false-positive" TCA result. This eye showed very significant cup enlargement by TCA ($CAREA^{disc}$ = 0.819 mm^2), but showed no change by stereophotography or SAP GPA.

The parameter with the nominal best diagnostic accuracy (considering sensitivity based on disc and/or GPA criterion) for each of the MEH-data determined specificity cutoffs (0.90, 0.95, and 0.99) was $CAREA^{disc}$. We therefore applied this parameter (for largest area cluster and significant pixel depth change > 0 μm) using the previously determined cutoffs to the 210 DIGS nonprogressing eyes. Specificities in these eyes were 0.464 (95% CI, 0.394–0.534) with the 0.90 cutoff (0.036 mm^2), 0.570 (95% CI, 0.500–0.640) with the 0.95 cutoff (0.055 mm^2), and 0.647 (95% CI, 0.580–0.718) with the 0.99 cutoff (0.074 mm^2). Specificities in the DIGS longitudinal healthy eyes using these same cutoffs were 0.809 (95% CI, 0.618–1.00), 0.857 (95% CI, 0.684–1.00), and 1.00 (95% CI, 0.976–1.00), respectively (i.e., specificities were very different between "nonprogressing" and healthy groups).

Finally, we use ANOVA to compare the output for 35 parameters (all the study parameters based on the largest area superpixel cluster only) among eyes progressing by disc *and/or* GPA, nonprogressing eyes, and longitudinally healthy eyes. Significant differences among groups were found for most parameters when significant retinal height change (depth of defect) was not specified or when the specified depth of defect was shallow (i.e., ≥20 μm) and in almost every case, pair-wise comparisons (Tukey-Kramer HSD, α = 0.05) identified differences between progressing and healthy eyes, only. For almost all parameters, values from nonprogressing eyes fell between those for progressing and healthy eyes and in two cases ($CSIZE^{disc}$ and $CAREA^{disc}$ when all significant superpixels were included in the identified clusters), values from nonprogressing eyes exceeded those from progressing eyes. This information is presented in Table 4, which also shows results for eyes progressing by disc regardless of GPA result. In many cases, TCA detected slightly larger areas of change in these eyes than in eyes progressed by disc and/or GPA. These values were not compared directly, because the groups were not independent (the group of 20 eyes progressed by disc are included in the group of 36 eyes progressed by either criterion).

Discussion

The present study introduces new TCA parameters and suggests parameter cutoffs for detecting progression in eyes with suspected or known primary open-angle glaucoma. Cutoffs were derived from a large number of permuted topographical sequences obtained from a somewhat small number of healthy eyes, and these derived cutoffs resulted in acceptable classification (described by sensitivity and specificity) when applied to known progressing and stable eyes. When the best-performing cutoffs were applied to longitudinal topographic series obtained from patient eyes observed for four or more years and showing no evidence of progression based on SAP or stereophotographic assessment (i.e., current standards for progression detection), specificities were poor to moderate (e.g., from 0.464 for $CAREA^{disc}$, with the 0.90 specificity cutoff of 0.036 mm^2, to 0.647, with the 0.99 specificity cutoff of 0.074 mm^2). In addition, outputs from progressing and nonprogressing eyes for all parameters investigated were statistically similar and TCA cluster size measurements from nonprogressing eyes fell between those from progressing and healthy eyes. The latter two results suggest that true change, undetectable by current progression assessment techniques, occurred in some of these eyes. Because our sensitivity and specificity test sets were small (i.e., 36 eyes and 20 eyes for sensitivity and 21 eyes for specificity), it is important that some of the recommended TCA parameter cutoffs presented herein be tested in independent data sets, to better characterize their performance.

Initial studies using (and developing) TCA, by Chauhan and et al.,[6,8] suggested that a progression event be defined as a repeatable significant change of ≥20 contiguous superpixels. This limit was derived based on the fact that <5% of 37 healthy eyes, followed longitudinally, showed repeatable (three or more times) clusters of ≥20 progressing superpixels. This suggestion has since been refined by including measurements within the disc and measurements of depth of defect. Recently, Artes and Chauhan (Artes PH, et al. *IOVS* 2006;47:ARVO E-Abstract 4349) investigated the TCA change in glaucomatous ($n = 172$) and healthy eyes ($n = 60$) followed for approximately 8 years. These authors described TCA change based on cluster size (e.g., ≥1%, ≥5%, and ≥10% of disc area) and cluster depth (e.g., ≥0, ≥50, and ≥200 μm) and compared survival rates (percentage of eyes progressing) to identify cluster characteristics that provided the best separation between glaucomatous and healthy groups. Results suggested that the ideal parameters for separating these two groups were small clusters (between 1% and 2% of disc areas) with shallow depth changes (20–50 μm). When clusters were larger and depth changes were greater, separation success decreased. It is important to note that this study did not rely on a reference standard for progression and it is expected that a significant percentage of glaucomatous eyes were not actually progressing. Theoretically, this fact could decrease the diagnostic accuracy of the identified cutoffs. However, in the present study, we found generally good performance with similar cutoffs (that were derived differently), although we did not combine area and depth-of-defect measurements. Other recent studies have suggested that effective TCA cutoffs might need adjustment based on other factors such as disease severity (Chauhan BC, et al. *IOVS* 2007;48:ARVO E-Abstract 3330) and optic disc phenotype.[18]

Newer techniques for detecting image-wide change in HRT topographic series have recently been described. One technique, statistical image mapping (SIM), correctly identified a larger number of known progressing eyes (21/30 OHT eyes that developed repeatable VF loss defined by change in AGIS score over follow-up) than did TCA (16/30) and regression of rim area (15/30). A similar number of longitudinally healthy eyes were correctly identified by all three techniques (18/20, 17/20, and 18/20 for SIM, TCA, and rim area regression, respectively).[11] In the SIM study, TCA progression was defined as ≥20 red superpixels within the contour line. Other recent techniques under development apply different image analysis techniques, such as proper orthogonal decomposition. Preliminary analyses using these techniques suggest that their performance for discriminating between progressing and longitudinal normal eyes is similar to that of TCA (Balasubramanian M, et al. *IOVS* 2007;48:ARVO E-Abstract 3331; Balasubramanian M, et al. *IOVS* 2008;49:ARVO E-Abstract 3625).

In the present study, and in others, TCA performed acceptably when simply counting pixels in the largest contiguous cluster. However, we expect that performance could be improved if the locations of the largest clusters were considered (although this would require more sophisticated automation). For instance, some large clusters might fall on vessels or the largest cluster might not necessarily be the most informative one based on location (e.g., it may fall on the nasal rim or in the parapapillary region away from arcuate nerve fiber bundles). In addition, we may need to consider change in the positive direction because localized decreases in retinal height due to tissue loss may be accompanied by increases in retinal height caused by possible tissue repositioning[19] or possible restructuring of the optic disc by glial cells.[20] The interaction between positive and negative change in retinal height should be the subject of future study.

It can be argued that developing TCA cutoffs for the binary classification of progressing and nonprogressing eyes creates an artificial, single-event–related situation that could be misinterpreted clinically and could result in over- or undertreatment. However, recent studies suggest that at least some guidance in TCA interpretation is necessary. Results from one study suggested that agreement is only moderate to good among glaucoma fellowship-trained

clinicians when subjectively judging progression from printed TCA images series where no cluster size information is available.[21] Results from the same data set suggest that agreement is poor between clinicians' judgment of progression based on TCA images and progression defined based on masked assessment of stereophotographs (see also Refs. 8, [22]). The provision of objectively defined cutoffs probably could standardize TCA interpretation; however, such cutoffs should not be used in isolation from other clinical data, because different criteria should be considered for different disease severities and risk levels. Development of disease severity and risk-based criteria for identifying TCA-based progression should be topics for future research.

In the present study, a limited sample was used to test sensitivity. The size of the sample most likely reflects the lack of a currently available sensitive and accurate gold standard to detect change caused by a slowly progressing disease in mostly treated patients. However, the number of progressed eyes in the present study was similar to that reported in previous studies. The specificity test set also was limited in size, in part because it can be difficult and costly to recruit and retain, over a long period, healthy participants who are not at risk for disease. Because of the small sample size and as suggested previously, it is important that these results be replicated in independent data sets to investigate their generalizability.

We believe it is important to determine whether HRT TCA can detect progression that has been detected by either optic disc assessment or visual field assessment, because both of these techniques are current clinical standards that inform treatment. However, because previous evidence suggests poor agreement between progression detected based on optic disc assessment (e.g., by HRT, stereophotography) and progression detected based on visual field testing,[8,10,12] we conducted a subset analysis of TCA sensitivity in eyes that progressed by optic disc assessment regardless of visual field assessment. In general, results were similar. For instance, sensitivities of $CAREA^{disc}$ (largest area cluster, significant pixel depth change > 0 μm) at the 0.90, 0.95, and 0.99 specificity cutoffs in the subset of the 20 eyes that progressed by stereophotograph assessment were 0.750 using the 0.90 cutoff, 0.600 using the 0.95 cutoff, and 0.550 using the 0.99 cutoff. Sensitivities in eyes progressing by either stereophotograph assessment and/or SAP GPA (n = 36) using these same cutoffs were 0.778, 0.639, and 0.611, respectively. These results suggest that TCA sensitivity probably does not improve when the gold standard for progression is based on apparent photographic change of disc topography only. The observed small differences in sensitivity between progressed groups are most likely primarily attributable to the difference in the number of eyes considered. However, the results presented in Table 4 suggest that TCA detected slightly more change in eyes that progressed based on disc assessment compared with those progressed by disc assessment and/or GPA. This result is not entirely surprising, because eyes with visible progression by stereophotograph assessment probably have undergone more topographic change than eyes with functional progression that is undetectable by stereophotograph assessment.

Some studies have shown a significant but small cross-sectional effect of age on optic disc and retinal nerve fiber layer measurements in vivo (e.g., approximately 1% decrease in rim area every two years based on HRT measurements[23] and approximately 0.2 μm/year RNFL thinning based on optical coherence tomography and scanning laser polarimetry measurements[24–26]), although this effect is somewhat controversial.[27] This variable was not accounted for in the randomly assembled pseudolongitudinal series used to derive TCA cutoffs in the present study. Because of this, it is possible that the natural aging of longitudinally followed study participants contributed in part to the assumed disease-related change reported, possibly artificially increasing sensitivity and decreasing specificity of TCA parameters. However, average follow-up for progressing and nonprogressing eyes in the present study was a approximately 4 years with a maximum follow-up of 7.40 years, making significant age-related change unlikely in most if not all eyes. In addition, any small effect of age present in these relatively short

longitudinal series probably would be masked by the test–retest variability present in repeated HRT measurements.[28]

Finally, the HRT 1 examinations from the MEH healthy eyes used to derive the TCA parameter cutoffs were 10° scans, while the HRT-II examinations from the DIGS eyes used to evaluate diagnostic accuracy were 15° scans. The smaller retinal scan area of the 10° scans may have resulted in slightly lower cutoff values for the TCA parameters describing change anywhere within the whole field of view (i.e., parameters $CSIZE^{total}$, $CAREA^{total}$, and $CVOL^{total}$). If changes in the far-parapapillary area were prominent, it could have resulted in higher sensitivities and lower specificities in DIGS eyes for these parameters, due to low cutoff values. However, the specificity of these parameters was generally very high, with lower sensitivities. Also, cutoff values for these parameters are considerably larger than cutoffs for within-disc parameters (for example, $CSIZE^{total}$ cutoff is 164 superpixels compared to the $CSIZE^{disc}$ cutoff of 20 superpixels at 0.90 specificity of MEH eyes in Table 2). Although it is ideal to use scans with the same retinal area to derive and test full-image cutoff parameters, our results suggest that 10° and 15° scan areas generally are comparable for this purpose.

Conclusion

This study tested HRT TCA-based parameter cutoffs, developed based on specificity in a large number of permuted topographic series from healthy eyes, for detecting known glaucomatous progression. Overall, TCA performance using these new cutoffs was adequate. Results also showed that a significant number of glaucomatous and/or suspect eyes, that were apparently stable by current progression–detection techniques, showed significant TCA change when subjected to the derived cutoffs. We believe this finding provides some evidence that HRT TCA analysis can detect change earlier (or detect more subtle change) than both stereophotographic assessment and currently available visual field–based progression detection techniques (ideally, longer photographic and SAP follow-up of our patients is needed to confirm early TCA-detected progression). If this is the case, the current results provide additional support for the use of optical imaging data in clinical trials research.

Acknowledgments

The authors thank David P. Crabb (Department of Optometry and Visual Science, City University, London, UK) and David F. Garway-Heath (Glaucoma Research Unit, Moorfields Eye Hospital, London, UK) for their input and for providing the MEH longitudinal dataset for the analyses.

Supported by National Institutes of Health Grants EY011008 and EY008208 and participant incentive grants in the form of glaucoma medication at no cost from Alcon Laboratories Inc, Allergan, Pfizer Inc., and Santen, Inc.

References

1. Zangwill, L.; Medeiros, F.; Bowd, C.; Weinreb, R. Optic nerve imaging: recent advances. In: Grehn, F.; Stamper, R., editors. Glaucoma. Berlin: Springer-Verlag; 2004. p. 63-91.
2. Strouthidis N, Garway-Heath D. New developments in Heidelberg Retina Tomograph for glaucoma. Curr Opin Ophthalmol 2008;19:141–148. [PubMed: 18301288]
3. Repka MX, Quigley HA. The effect of age on normal human optic nerve fiber number and diameter. Ophthalmology 1989;96:26–32. [PubMed: 2919049]
4. Jonas JB, Muller-Bergh JA, Schlotzer-Schrehardt UM, Naumann GO. Histomorphometry of the human optic nerve. Invest Ophthalmol Vis Sci 1990;31:736–744. [PubMed: 2335441]
5. Kamal DS, Viswanathan AC, Garway-Heath DF, Hitchings RA, Poinoosawmy D, Bunce C. Detection of optic disc change with the Heidelberg retina tomograph before confirmed visual field change in ocular hypertensives converting to early glaucoma. Br J Ophthalmol 1999;83:290–294. [PubMed: 10365035]

6. Chauhan BC, Blanchard JW, Hamilton DC, LeBlanc RP. Technique for detecting serial topographic changes in the optic disc and peripapillary retina using scanning laser tomography. Invest Ophthalmol Vis Sci 2000;41:775–782. [PubMed: 10711693]
7. Kamal DS, Garway-Heath DF, Hitchings RA, Fitzke FW. Use of sequential Heidelberg retina tomograph images to identify changes at the optic disc in ocular hypertensive patients at risk of developing glaucoma. Br J Ophthalmol 2000;84:993–998. [PubMed: 10966952]
8. Chauhan BC, McCormick TA, Nicolela MT, LeBlanc RP. Optic disc and visual field changes in a prospective longitudinal study of patients with glaucoma: comparison of scanning laser tomography with conventional perimetry and optic disc photography. Arch Ophthalmol 2001;119:1492–1499. [PubMed: 11594950]
9. Tan JC, Hitchings RA. Approach for identifying glaucomatous optic nerve progression by scanning laser tomography. Invest Ophthalmol Vis Sci 2003;44:2621–2626. [PubMed: 12766065]
10. Artes PH, Chauhan BC. Longitudinal changes in the visual field and optic disc in glaucoma. Prog Retinal Eye Res 2005;24:333–354.
11. Patterson AJ, Garway-Heath DF, Strouthidis NG, Crabb DP. A new statistical approach for quantifying change in series of retinal and optic nerve head topography images. Invest Ophthalmol Vis Sci 2005;46:1659–1667. [PubMed: 15851566]
12. Strouthidis NG, Scott A, Peter NM, Garway-Heath DF. Optic disc and visual field progression in ocular hypertensive subjects: detection rates, specificity, and agreement. Invest Ophthalmol Vis Sci 2006;47:2904–2910. [PubMed: 16799032]
13. Fayers T, Strouthidis NG, Garway-Heath DF. Monitoring glaucomatous progression using a novel Heidelberg Retina Tomograph event analysis. Ophthalmology 2007;114:1973–1980. [PubMed: 17662455]
14. Kalaboukhova L, Fridhammar V, Lindblom B. Glaucoma follow-up by the Heidelberg retina tomograph–new graphical analysis of optic disc topography changes. Graefes Arch Clin Exp Ophthalmol 2006;244:654–662. [PubMed: 16220279]
15. Balasubramanian, M.; Bowd, C.; Zangwill, L. Algorithms for detecting glaucomatous structural changes in the optic nerve head. In: Rajendra Acharya, U.; Ng, EK.; Suri, JS., editors. Image Modeling of the Human Eye. Boston: Artech House; 2008. p. 163-204.
16. Anderson, DR.; Patella, VM. Automated Static Perimetry. Vol. 2. St. Louis: Mosby; 1999.
17. Leske MC, Heijl A, Hyman L, Bengtsson B. Early Manifest Glaucoma Trial: design and baseline data. Ophthalmology 1999;106:2144–2153. [PubMed: 10571351]
18. Nicolela MT, McCormick TA, Drance SM, Ferrier SN, LeBlanc RP, Chauhan BC. Visual field and optic disc progression in patients with different types of optic disc damage: a longitudinal prospective study. Ophthalmology 2003;110:2178–2184. [PubMed: 14597527]
19. Burgoyne CF, Quigley HA, Thompson HW, Vitale S, Varma R. Early changes in optic disc compliance and surface position in experimental glaucoma. Ophthalmology 1995;102:1800–1809. [PubMed: 9098280]
20. Wirtschafter JD. Optic nerve axons and acquired alterations in the appearance of the optic disc. Trans Am Ophthalmol Soc 1983;81:1034–1091. [PubMed: 6203209]
21. Vizzeri G, Weinreb RN, Martinez de la Casa JM, et al. Clinicians agreement in establishing glaucomatous progression using the HRT confocal scanning laser ophthalmoscope. Ophthalmology. 2008 Nov 15;[Epub ahead of print]
22. Kourkoutas D, Buys YM, Flanagan JG, Hatch WV, Balian C, Trope GE. Comparison of glaucoma progression evaluated with Heidelberg retina tomograph II versus optic nerve head stereophotographs. Can J Ophthalmol 2007;42:82–88. [PubMed: 17361246]
23. Garway-Heath DF, Wollstein G, Hitchings RA. Aging changes of the optic nerve head in relation to open angle glaucoma. Br J Ophthalmol 1997;81:840–845. [PubMed: 9486023]
24. Bowd C, Zangwill LM, Blumenthal EZ, et al. Imaging of the optic disc and retinal nerve fiber layer: the effects of age, optic disc area, refractive error, and gender. J Opt Soc Am A Opt Image Sci Vis 2002;19:197–207. [PubMed: 11778725]
25. Budenz DL, Anderson DR, Varma R, et al. Determinants of normal retinal nerve fiber layer thickness measured by Stratus OCT. Ophthalmology 2007;114:1046–1052. [PubMed: 17210181]

26. Parikh RS, Parikh SR, Sekhar GC, Prabakaran S, Babu JG, Thomas R. Normal age-related decay of retinal nerve fiber layer thickness. Ophthalmology 2007;114:921–926. [PubMed: 17467529]

27. Varma R, Tielsch JM, Quigley HA, et al. Race-, age-, gender-, and refractive error-related differences in the normal optic disc. Arch Ophthalmol 1994;112:1068–1076. [PubMed: 8053821]

28. DeLeon Ortega JE, Sakata LM, Kakati B, et al. Effect of glaucomatous damage on repeatability of confocal scanning laser ophthalmoscope, scanning laser polarimetry, and optical coherence tomography. Invest Ophthalmol Vis Sci 2007;48:1156–1163. [PubMed: 17325159]

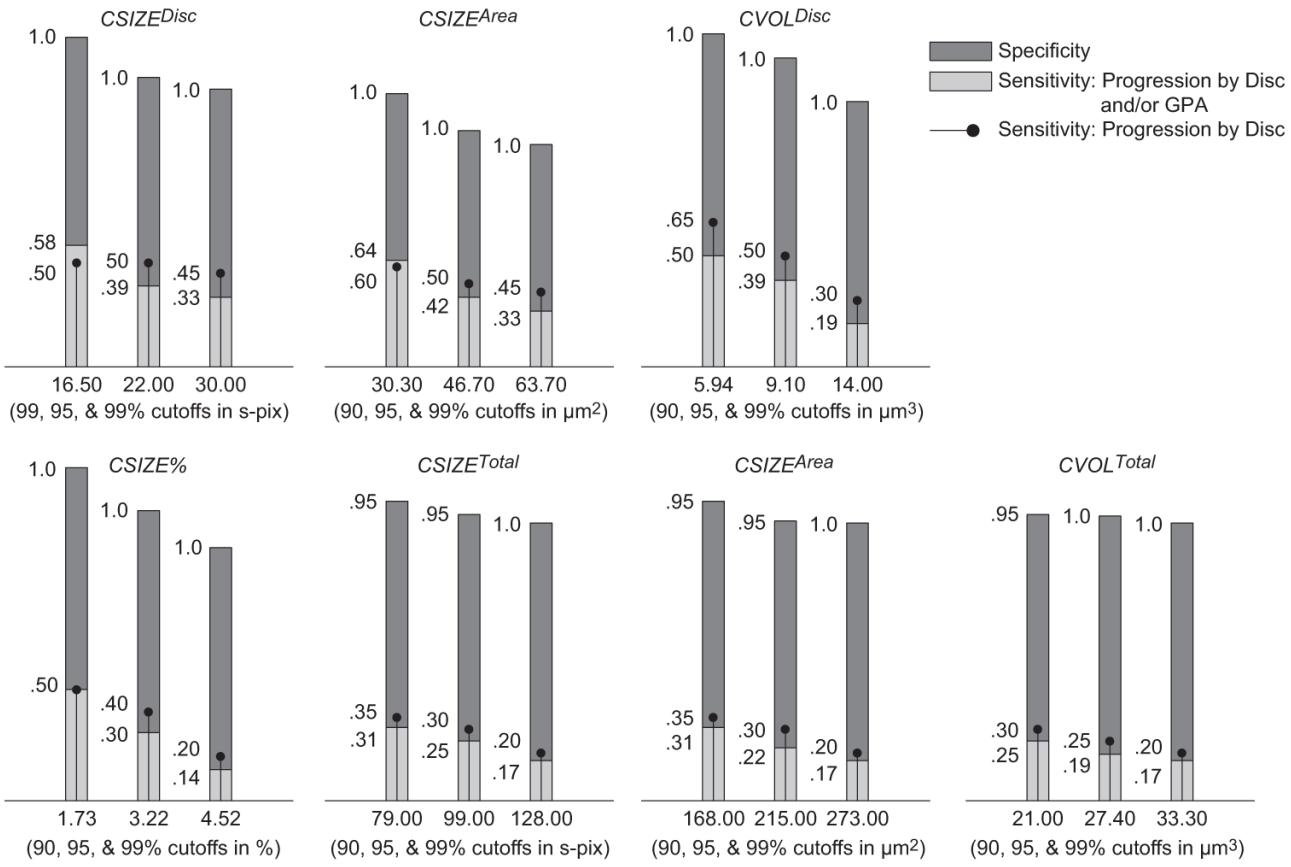

Figure 1.

Sensitivities, specificities, and cutoffs for TCA parameters at 0.99, 0.95, and 0.90 specificity cutoffs (determined using permuted longitudinal data with 1000 permutations) for largest area superpixel clusters. Only pixels with depth change from baseline ≥ 50 μm were considered outside normal limits. Although HRT measurements are generally expressed in millimeters, the cutoff values are expressed in micrometers, to prevent rounding to zero in some cases.

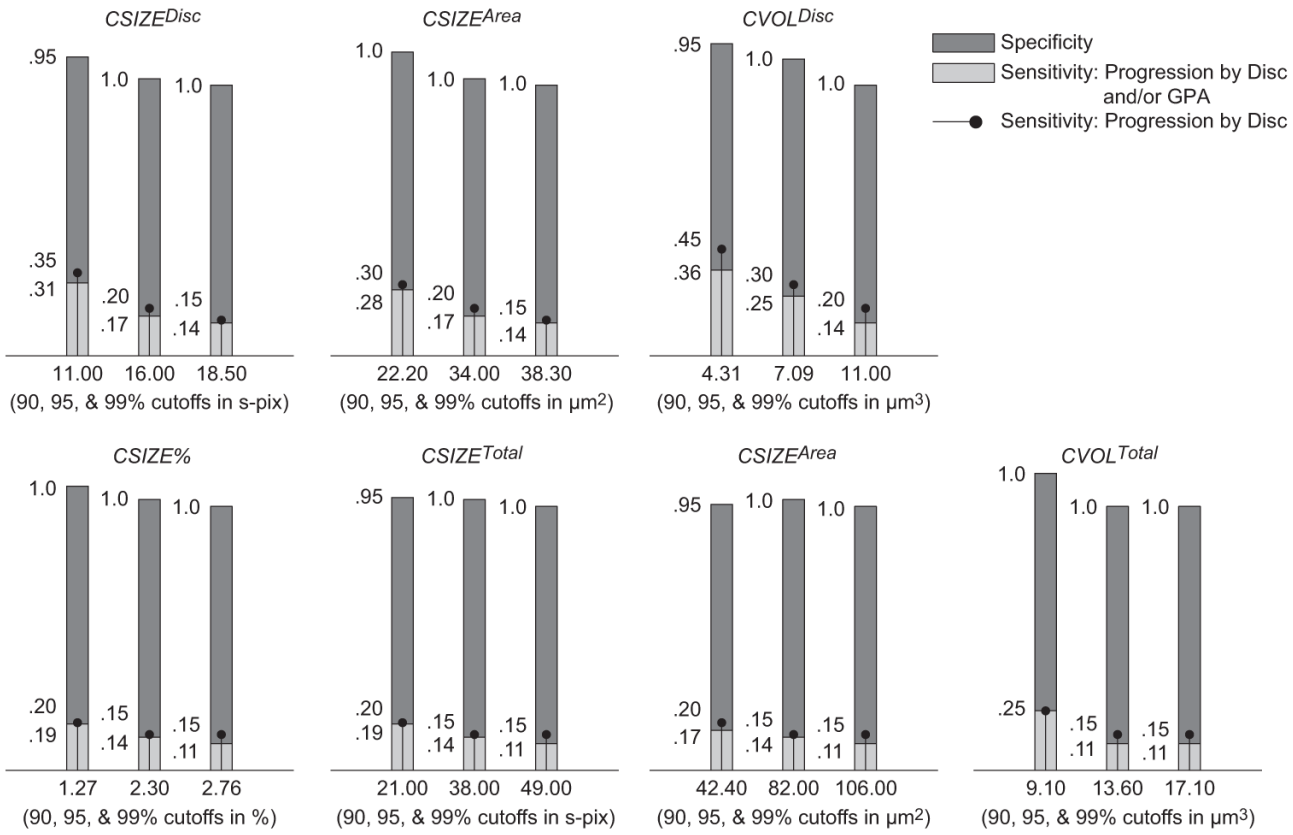

Figure 2.

Sensitivities, specificities, and cutoffs for TCA parameters at 0.99, 0.95, and 0.90 specificity cutoffs (determined using permuted longitudinal data with 1000 permutations) for largest area superpixel clusters. Only pixels with depth change from baseline ≥ 100 μm were considered outside normal limits.

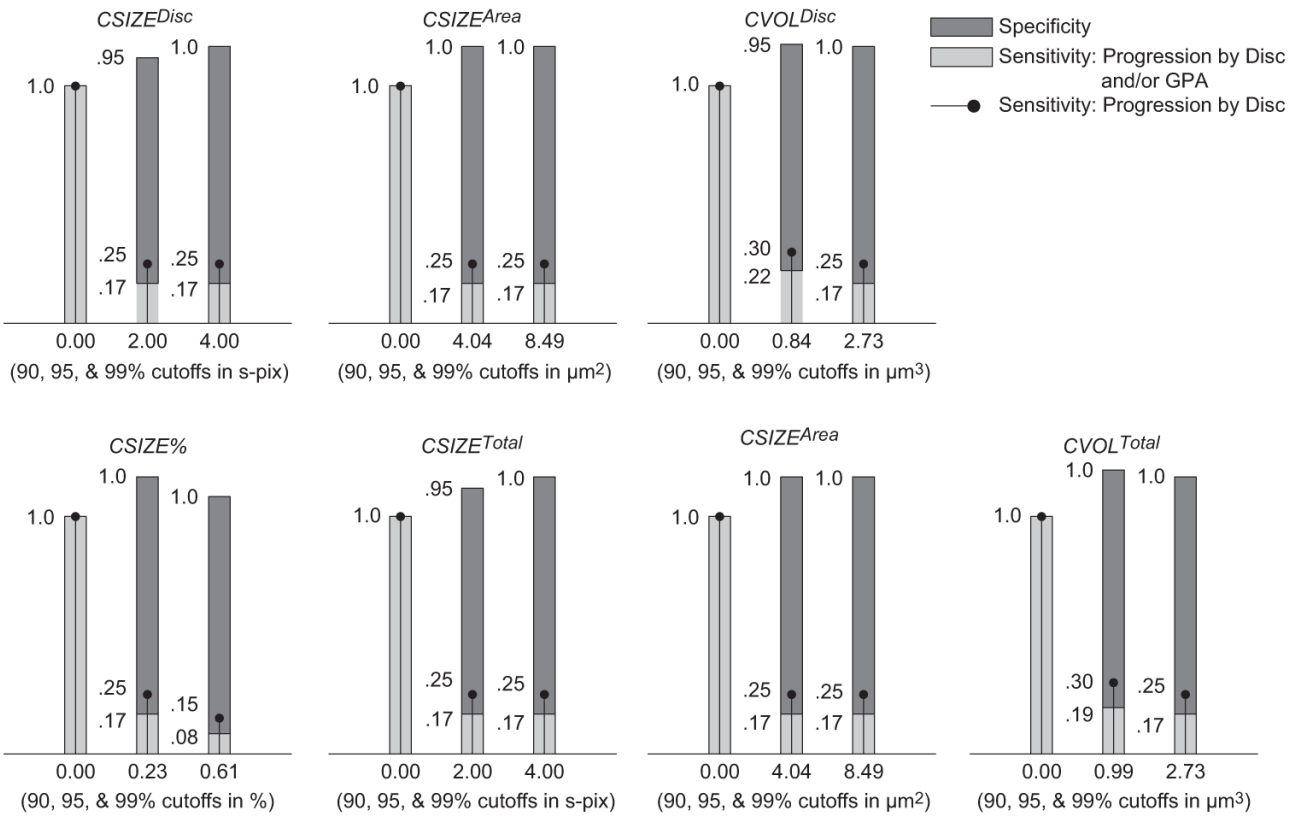

Figure 3.

Sensitivities, specificities and cutoffs for TCA parameters at 0.99, 0.95, and 0.90 specificity cutoffs (determined using permuted longitudinal data with 1000 permutations) for largest area superpixel clusters. Only pixels with depth change from baseline ≥ 200 μm were considered outside normal limits.

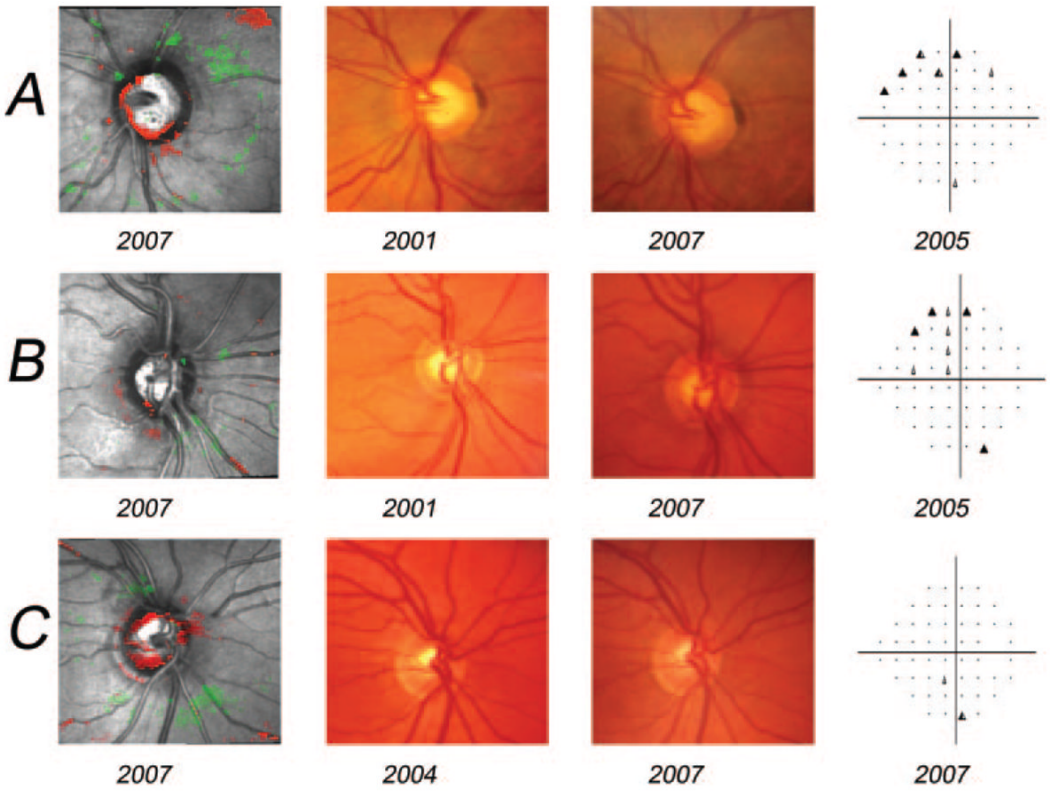

Figure 4.

Examples of agreement for detecting progression among TCA analysis, stereophotography assessment and SAP GPA. (**A**) An example of a true-positive TCA result. This eye progressed by stereophotograph assessment, SAP GPA and TCA $CAREA^{disc}$ (using the 0.90 specificity cutoff of ≥0.036 mm^2). Inferior rim thinning was apparent in both the TCA image ($CAREA^{disc}$ = 0.252 mm^2) and the stereophotograph pair. This change is reflected in significant superior hemifield change measured by GPA. (**B**) An example of a false-negative TCA result. This eye progressed by stereophotograph assessment and SAP GPA, but not by TCA. Inferior rim thinning is apparent in the stereophotograph pair and reflected in significant superior hemifield change by GPA. However, the TCA image shows little clustered change ($CAREA^{disc}$ = 0.011 mm^2). (**C**) A "false-positive" TCA result. This eye showed very significant cup enlargement by TCA ($CAREA^{disc}$ = 0.819 mm^2) but showed no change by stereophotography or SAP GPA.

Table 1

Population Summary of the Progressed and Nonprogressed Patient Datasets from the UCSD Diagnostic Innovations in Glaucoma Study

	DIGS Eyes Progressed by Disc and/or GPA	DIGS Eyes Progressed by Disc	DIGS Eyes Nonprogressed
Eyes (*n*)	36	20	210
Subjects (*n*)	33	20	148
Age (y), mean (95% CI)	70.37 (67.26–73.48)	67.65 (63.99–71.31)	66.24 (64.24–68.24)
HRT exams (*n*), median (range)	5 (4–8)	5 (4–8)	4 (4–8)
HRT follow-up (y), median (range)	4.13 (2.38–6.96)	4.36 (2.38–6.96)	3.59 (1.65–7.40)
SAP MD at baseline (dB), mean (95% CI)	−3.65 (−5.45–−1.84)	−4.34 (−7.35–−1.33)	−1.72 (−2.16–−1.28)
SAP PSD at baseline (dB), mean (95% CI)	4.19 (2.87–5.51)	5.32 (3.10–7.54)	2.47 (2.18–2.76)
Abnormal disc by photography only at baseline, *n* (%)	12 (33.3)	6 (30.0)	54 (25.7)
Abnormal visual field only at baseline, *n* (%)	4 (11.1)	1 (5.0)	28 (13.33)
Abnormal disc and abnormal visual field at baseline, *n* (%)	15 (41.7)	9 (45.0)	41 (19.52)
Normal disc and normal visual field at baseline, *n* (%)	5 (13.9)	4 (20.0)	87 (41.43)

Table 2

Sensitivities, Specificities, and Cutoffs for TCA Parameters at the Three Specificity Cutoffs, with Pixels Outside Normal Limits Considered, Regardless of Depth of Change from Baseline

		Largest Area Cluster (95% CI)			Largest Volume Cluster (95% CI)		
Parameter	**Sensitivity**	**0.99 Specificity Cutoff**	**0.95 Specificity Cutoff**	**0.90 Specificity Cutoff**	**0.99 Specificity Cutoff**	**0.95 Specificity Cutoff**	**0.90 Specificity Cutoff**
CSIZE^{disc}	Sensitivity by disc or GPA	0.639 (0.468–0.810)	0.667 (0.499–0.834)	0.722 (0.562–0.882)	0.639 (0.468–0.810)	0.667 (0.499–0.834)	0.722 (0.562–0.882)
	Sensitivity by disc	0.600 (0.360–0.840)	0.600 (0.360–0.840)	0.750 (0.535–0.965)	0.600 (0.360–0.840)	0.600 (0.360–0.840)	0.750 (0.535–0.965)
	Specificity	0.952 (0.837–1.00)	0.809 (0.618–1.00)	0.809 (0.618–1.00)	0.952 (0.838–1.00)	0.809 (0.618–1.00)	0.809 (0.618–1.00)
	Cutoff	35.0 s-pixels	27.0 s-pixels	20.0 s-pixels	35.0 s-pixels	27.0 s-pixels	20.0 s-pixels
CAREA^{disc}	Sensitivity by disc or GPA	0.611 (0.438–0.784)	0.639 (0.468–0.810)	0.778 (0.628–0.928)	0.611 (0.438–0.784)	0.667 (0.499–0.834)	0.778 (0.628–0.927)
	Sensitivity by disc	0.550 (0.307–0.793)	0.600 (0.360–0.840)	0.750 (0.535–0.965)	0.550 (0.307–0.793)	0.600 (0.360–0.840)	0.750 (0.535–0.965)
	Specificity	1.00 (0.976–1.00)	0.857 (0.684–1.00)	0.809 (0.618–1.00)	1.00 (0.976–1.00)	0.857 (0.683–1.00)	0.809 (0.618–1.00)
	Cutoff	0.074 mm^2	0.055 mm^2	0.036 mm^2	0.074 mm^2	0.055 mm^2	0.036 mm^2
CVOL^{disc}	Sensitivity by disc or GPA	0.250 (0.094–0.405)	0.417 (0.242–0.592)	0.611 (0.438–0.784)	0.250 (0.095–0.405)	0.444 (0.268–0.621)	0.639 (0.468–0.810)
	Sensitivity by disc	0.350 (0.116–0.584)	0.550 (0.307–0.793)	0.600 (0.360–0.840)	0.350 (0.116–0.584)	0.600 (0.360–0.840)	0.6500 (0.416–0.884)
	Specificity	1.00 (0.976–1.00)	1.00 (0.976–1.00)	0.952 (0.838–1.00)	1.00 (0.976–1.00)	1.00 (0.976–1.00)	0.952 (0.838–1.00)
	Cutoff	0.015 mm^3	0.010 mm^3	0.006 mm^3	0.015 mm^3	0.010 mm^3	0.006 mm^3
CSIZE%	Sensitivity by disc or GPA	0.389 (0.216–0.562)	0.500 (0.323–0.677)	0.750 (0.595–0.905)	0.389 (0.216–0.562)	0.500 (0.322–0.677)	0.750 (0.595–0.905)
	Sensitivity by disc	0.350 (0.116–0.584)	0.450 (0.207–0.693)	0.750 (0.535–0.965)	0.350 (0.116–0.584)	0.450 (0.207–0.693)	0.750 (0.535–0.965)
	Specificity	1.00 (0.976–1.00)	1.00 (0.976–1.00)	0.809 (0.618–1.00)	1.00 (0.976–1.00)	1.00 (0.976–1.00)	0.809 (0.618–1.00)
	Cutoff	5.21%	3.98%	1.96%	5.21%	3.98%	1.96%
CSIZE^{total}	Sensitivity by disc or GPA	0.333 (0.165–0.501)	0.389 (0.216–0.562)	0.500 (0.323–0.677)	0.333 (0.165–0.501)	0.389 (0.215–0.562)	0.472 (0.295–0.649)
	Sensitivity by disc	0.250 (0.035–0.465)	0.350 (0.116–0.584)	0.500 (0.256–0.744)	0.250 (0.035–0.465)	0.350 (0.116–0.584)	0.450 (0.207–0.693)
	Specificity	1.00 (0.976–1.00)	1.00 (0.976–1.00)	0.809 (0.618–1.00)	1.00 (0.976–1.00)	1.00 (0.976–1.00)	0.809 (0.618–1.00)
	Cutoff	164.0 s-pixels	135.0 s-pixels	120.0 s-pixels	164.0 s-pixels	135.0 s-pixels	120.0 s-pixels
CAREA^{total}	Sensitivity by disc or GPA	0.333 (0.165–0.501)	0.444 (0.268–0.621)	0.500 (0.323–0.677)	0.417 (0.242–0.592)	0.417 (0.242–0.592)	0.444 (0.268–0.621)
	Sensitivity by disc	0.250 (0.035–0.465)	0.400 (0.160–0.640)	0.450 (0.207–0.693)	0.250 (0.035–0.465)	0.350 (0.116–0.584)	0.350 (0.116–0.584)
	Specificity	1.00 (0.976–1.00)	1.00 (0.976–1.00)	0.952 (0.837–1.00)	1.00 (0.976–1.00)	1.00 (0.976–1.00)	0.952 (0.837–1.00)
	Cutoff	0.355 mm^2	0.288 mm^2	0.260 mm^2	164.0 s-pixels	135.0 s-pixels	120.0 s-pixels
CVOL^{total}	Sensitivity by disc or GPA	0.222 (0.072–0.372)	0.222 (0.072–0.372)	0.333 (0.165–0.501)	0.222 (0.072–0.372)	0.222 (0.072–0.372)	0.333 (0.165–0.501)
	Sensitivity by disc	0.250 (0.035–0.465)	0.250 (0.035–0.465)	0.350 (0.116–0.584)	0.250 (0.035–0.465)	0.250 (0.035–0.465)	0.350 (0.116–0.584)
	Specificity	1.00 (0.976–1.00)	1.00 (0.976–1.00)	0.952 (0.837–1.00)	1.00 (0.976–1.00)	1.00 (0.976–1.00)	0.952 (0.837–1.00)
	Cutoff	0.040 mm^3	0.033 mm^3	0.025 mm^3	0.040 mm^3	0.033 mm^3	0.025 mm^3

Cutoffs were determined using permuted longitudinal healthy data with 1000 permutations. *CSIZE*^{disc}, the number of superpixels (s-pixels) within a cluster within the optic disc margin; *CAREA*^{disc}, area of a cluster (mm^2) within the optic disc margin; *CVOL*^{disc}, volume of a cluster (mm^3) within the optic disc margin; *CSIZE%*, cluster size in superpixels expressed as percentage of optic disc area; *CSIZE*^{total}, the number of superpixels within the whole image field of view; *CAREA*^{total}, area of cluster (mm^2) within the whole image field of view; *CVOL*^{total}, volume of a cluster (mm^3) within the whole image field of view.

Table 3

Sensitivities, Specificities, and Cutoffs for TCA Parameters at the Three Specificity Cutoffs, with Only Pixels with Depth Change from Baseline ≥ 20 μm Considered Outside Normal Limits

		Largest Area Cluster (95% CI)			Largest Volume Cluster (95% CI)		
Parameter	**Sensitivity**	**0.99 Specificity Cutoff**	**0.95 Specificity Cutoff**	**0.90 Specificity Cutoff**	**0.99 Specificity Cutoff**	**0.95 Specificity Cutoff**	**0.90 Specificity Cutoff**
CSIZE^{disc}	Sensitivity by disc or GPA	0.472 (0.295–0.649)	0.639 (0.468–0.810)	0.722 (0.562–0.882)	0.472 (0.295–0.649)	0.611 (0.438–0.784)	0.722 (0.562–0.882)
	Sensitivity by disc	0.500 (0.256–0.744)	0.600 (0.360–0.840)	0.700 (0.474–0.923)	0.500 (0.256–0.744)	0.600 (0.360–0.840)	0.700 (0.474–0.923)
	Specificity	1.00 (0.976–1.00)	0.809 (0.618–1.00)	0.809 (0.618–1.00)	1.00 (0.976–1.00)	0.809 (0.618–1.00)	0.809 (0.618–1.00)
	Cutoff	37.5 s-pixels	26.5 s-pixels	19.5 s-pixels	37.5 s-pixels	26.5 s-pixels	19.5 s-pixels
CAREA^{disc}	Sensitivity by disc or GPA	0.472 (0.295–0.649)	0.639 (0.468–0.810)	0.750 (0.595–0.905)	0.444 (0.268–0.621)	0.639 (0.468–0.810)	0.750 (0.595–0.905)
	Sensitivity by disc	0.500 (0.256–0.744)	0.600 (0.360–0.840)	0.700 (0.474–0.923)	0.500 (0.256–0.744)	0.600 (0.360–0.840)	0.700 (0.474–0.923)
	Specificity	1.00 (0.976–1.00)	0.904 (0.755–1.00)	0.809 (0.618–1.00)	1.00 (0.976–1.00)	0.905 (0.755–1.00)	0.809 (0.618–1.00)
	Cutoff	0.079 mm^2	0.054 mm^2	0.036 mm^2	0.079 mm^2	0.054 mm^2	0.036 mm^2
CVOL^{disc}	Sensitivity by disc or GPA	0.250 (0.095–0.405)	0.389 (0.216–0.562)	0.556 (0.379–0.732)	0.250 (0.095–0.405)	0.444 (0.268–0.621)	0.611 (0.438–0.784)
	Sensitivity by disc	0.350 (0.116–0.584)	0.500 (0.256–0.744)	0.550 (0.307–0.793)	0.350 (0.116–0.584)	0.600 (0.360–0.840)	0.6500 (0.416–0.844)
	Specificity	1.00 (0.976–1.00)	1.00 (0.976–1.00)	0.952 (0.837–1.00)	1.00 (0.976–1.00)	1.00 (0.976–1.00)	0.952 (0.837–1.00)
	Cutoff	0.015 mm^3	0.010 mm^3	0.006 mm^3	0.015 mm^3	0.010 mm^3	0.006 mm^3
CSIZE%	Sensitivity by disc or GPA	0.278 (0.118–0.438)	0.417 (0.242–0.592)	0.722 (0.562–0.882)	0.306 (0.141–0.470)	0.417 (0.242–0.592)	0.722 (0.562–0.882)
	Sensitivity by disc	0.300 (0.074–0.526)	0.450 (0.207–0.693)	0.700 (0.474–0.923)	0.350 (0.116–0.584)	0.450 (0.207–0.693)	0.700 (0.474–0.923)
	Specificity	1.00 (0.976–1.00)	1.00 (0.976–1.00)	0.809 (0.618–1.00)	1.00 (0.976–1.00)	1.00 (0.976–1.00)	0.809 (0.618–1.00)
	Cutoff	5.28%	3.83%	1.96%	5.28%	3.83%	1.96%
CSIZE^{total}	Sensitivity by disc or GPA	0.278 (0.118–0.438)	0.361 (0.190–0.532)	0.417 (0.242–0.592)	0.278 (0.118–0.438)	0.361 (0.190–0.532)	0.417 (0.242–0.592)
	Sensitivity by disc	0.200 (0–0.400)	0.300 (0.074–0.526)	0.350 (0.116–0.584)	0.200 (0–0.400)	0.300 (0.074–0.526)	0.350 (0.116–0.584)
	Specificity	1.00 (0.976–1.00)	1.00 (0.976–1.00)	1.00 (0.976–1.00)	1.00 (0.976–1.00)	1.00 (0.976–1.00)	1.00 (0.976–1.00)
	Cutoff	163.5 s-pixels	131.0 s-pixels	116.5 s-pixels	163.5 s-pixels	131.0 s-pixels	115.5 s-pixels
CAREA^{total}	Sensitivity by disc or GPA	0.2778 (0.118–0.438)	0.333 (0.165–0.501)	0.417 (0.242–0.592)	0.278 (0.118–0.438)	0.333 (0.165–0.501)	0.417 (0.242–0.592)
	Sensitivity by disc	0.200 (0–0.400)	0.250 (0.035–0.465)	0.300 (0.074–0.526)	0.200 (0–0.400)	0.250 (0.035–0.465)	0.300 (0.074–0.526)
	Specificity	1.00 (0.976–1.00)	1.00 (0.976–1.00)	1.00 (0.976–1.00)	1.00 (0.976–1.00)	1.00 (0.976–1.00)	1.00 (0.976–1.00)
	Cutoff	0.347 mm^2	0.280 mm^2	0.252 mm^2	0.347 mm^2	0.280 mm^2	0.248 mm^2
CVOL^{total}	Sensitivity by disc or GPA	0.194 (0.051–0.338)	0.222 (0.072–0.372)	0.333 (0.165–0.501)	0.194 (0.051–0.338)	0.222 (0.072–0.372)	0.333 (0.165–0.501)
	Sensitivity by disc	0.200 (0–0.400)	0.250 (0.035–0.465)	0.350 (0.116–0.584)	0.200 (0–0.400)	0.250 (0.035–0.465)	0.350 (0.116–0.584)
	Specificity	1.00 (0.976–1.00)	1.00 (0.976–1.00)	0.952 (0.837–1.00)	1.00 (0.976–1.00)	1.00 (0.976–1.00)	0.952 (0.837–1.00)
	Cutoff	0.039 mm^3	0.032 mm^3	0.025 mm^3	0.039 mm^3	0.032 mm^3	0.025 mm^3

Determination of cutoffs and parameter definitions are as described in Table 2.

Table 4

Comparison of TCA Measurements among Progressed, Nonprogressed, and Healthy Eyes for 35 Parameters

Required Superpixel Depth Change	Parameter	Progressed Eyes by Disc and/or GPA (n = 36)	Nonprogressed Eyes (n = 210)	Healthy Eyes (n = 21)	P	Progressed Eyes by disc (n = 20)
Superpixel change ≥ 0 μm	$CSIZE^{disc}$ (s-pixels)	57.9 (36.1–79.8)	44.2 (34.9–53.4)	9.3 (3.8–14.9)	**0.036***	68.0 (38.1–98.0)
	$CAREA^{disc}$ (mm^2)	0.144 (0.067–0.161)	0.096 (0.075–0.116)	0.018 (0–0.082)	**0.047***	0.143 (0.057–0.228)
	$CVOL^{disc}$ (mm^3)	0.013 (0.001–0.018)	0.001 (0.007–0.012)	0.002 (0–0.009)	0.071	0.018 (0.001–0.026)
	$CSIZE\%$	5.03 (2.90–7.17)	4.41 (3.50–5.32)	0.94 (0–3.81)	0.057	5.96 (2.70–9.23)
	$CSIZE^{total}$ (s-pixels)	157.8 (102.4–213.4)	163.4 (139.7–187.1)	60.3 (37.5–83.0)	**0.035**†	132.7 (68.2–197.2)
	$CAREA^{total}$ (mm^2)	0.327 (0.210–0.494)	0.344 (0.294–0.394)	0.123 (0–0.280)	**0.032**†	0.279 (0.144–0.414)
	$CVOL^{total}$ (mm^3)	0.028 (0.018–0.037)	0.022 (0.018–0.026)	0.007 (0.004–0.010)	**0.028***	0.025 (0.009–0.042)
Superpixel change ≥20 μm	$CSIZE^{disc}$ (s-pixels)	50.4 (29.0–71.8)	38.3 (29.9–46.8)	8.4 (3.0–13.8)	**0.036***	64.3 (25.1–103.5)
	$CAREA^{disc}$ (mm^2)	0.104 (0.060–0.149)	0.082 (0.063–0.101)	0.017 (0.006–0.027)	**0.049***	0.135 (0.053–0.217)
	$CVOL^{disc}$ (mm^3)	0.012 (0.006–0.017)	0.009 (0.007–0.010)	0.002 (0.001–0.003)	0.085	0.017 (0.006–0.027)
	$CSIZE\%$	4.60 (2.84–6.36)	3.82 (2.95–4.70)	0.84 (0.33–1.35)	0.062	5.63 (2.45–8.82)
	$CSIZE^{total}$ (s-pixels)	135.5 (87.5–183.6)	129.2 (107.1–150.9)	47.0 (28.9–65.0)	0.054	109.7 (45.7–173.6)
	$CAREA^{total}$ (mm^2)	0.280 (0.181–0.379)	0.272 (0.226–0.318)	0.096 (0.059–0.134)	0.052	0.230 (0.097–0.363)
	$CVOL^{total}$ (mm^3)	0.027 (0.016–0.037)	0.020 (0.016–0.023)	0.006 (0.003–0.009)	**0.024***	0.024 (0.008–0.040)
Superpixel change ≥ 50 μm	$CSIZE^{disc}$ (s-pixels)	33.8 (14.6–52.9)	20.7 (15.1–26.3)	2.7 (1.1–4.3)	**0.026***	49.6 (13.8–85.5)
	$CAREA^{disc}$ (mm^2)	0.070 (0.031–0.110)	0.044 (0.032–0.057)	0.005 (0.002–0.008)	**0.038***	0.104 (0.029–0.179)
	$CVOL^{disc}$ (mm^3)	0.010 (0.005–0.016)	0.006 (0.004–0.009)	0.001 (0.0002–0.001)	0.081	0.015 (0.006–0.025)
	$CSIZE\%$	3.05 (1.49–4.62)	2.07 (1.49–2.64)	0.27 (0.12–0.42)	**0.047***	4.30 (1.39–7.22)
	$CSIZE^{total}$ (s-pixels)	81.8 (41.7–121.8)	50.7 (39.7–61.8)	14.0 (3.3–24.7)	**0.013***	78.0 (17.0–139.10)
	$CAREA^{total}$ (mm^2)	0.170 (0.09–0.254)	0.108 (0.083–0.132)	0.029 (0–0.107)	**0.006***	0.164 (0.037–0.291)
	$CVOL^{total}$ (mm^3)	0.021 (0.011–0.031)	0.012 (0.009–0.014)	0.003 (0.0005–0.001)	**0.008**‡	0.022 (0.007–0.037)
Superpixel change ≥ 100 μm	$CSIZE^{disc}$ (s-pixels)	11.8 (5.4–18.2)	6.3 (3.7–9.0)	0.7 (0. 1.9)	0.114	18.1 (1.6–34.6)
	$CAREA^{disc}$ (mm^2)	0.025 (0.006–0.043)	0.018 (0.008–0.020)	0.001 (0.003)	0.136	0.038 (0.004–0.072)
	$CVOL^{disc}$ (mm^3)	0.005 (0.002–0.008)	0.003 (0.002–0.005)	0.003 (0–0.001)	0.297	0.008 (0.002–0.014)
	$CSIZE\%$	1.05 (0.34–1.77)	0.62 (0.37–0.88)	0.07 (0–0.17)	0.145	1.54 (0.22–2.87)
	$CSIZE^{total}$ (s-pixels)	20.7 (7.1–34.2)	9.9 (6.5–13.3)	2.9 (0–5.8)	**0.030***	20.1 (1.64–38.56)
	$CAREA^{total}$ (mm^2)	0.043 (0.015–0.071)	0.022 (0.014–0.029)	0.006 (0–0.012)	**0.042**	0.042 (0.004–0.081)
	$CVOL^{total}$ (mm^3)	0.008 (0.004–0.012)	0.004 (0.003–0.006)	0.001 (0–0.002)	0.115	0.008 (0.002–0.014)
Superpixel change ≥ 200 μm	$CSIZE^{disc}$ (s-pixels)	1.7 (0.3–3.2)	1.6 (0.6–2.7)	0.1 (0–0.39)	0.630	2.85 (0.1–5.6)
	$CAREA^{disc}$ (mm^2)	0.003 (0.001–0.006)	0.004 (0.001–0.006)	<0.001 (0–0.001)	0.644	0.006 (0.003–0.011)
	$CVOL^{disc}$ (mm^3)	0.002 (0.0003–0.003)	0.001 (0.0005–0.002)	<0.0001 (0–0.003)	0.603	0.002 (0.0001–0.005)
	$CSIZE\%$	0.15 (0.02–0.28)	0.16 (0.06–0.26)	0.01 (0–0.02)	0.621	0.26 (0.02–0.49)
	$CSIZE^{total}$ (s-pixels)	2.0 (0.4–3.6)	1.8 (0.7–2.8)	0.1 (0–0.3)	0.571	2.8 (0.1–5.6)
	$CAREA^{total}$ (mm^2)	0.004 (0–0.009)	0.004 (0–0.006)	0.001 (0–0.007)	0.593	0.006 (0.0003–0.011)
	$CVOL^{total}$	0.002 (0–0.004)	0.001 (0–0.002)	<0.0001 (0–0.0001)	0.556	0.002 (0.0001–0.005)

Shown is the largest area cluster when the required total height change from baseline for each pixel was ≥0, ≥20, ≥50, ≥100, and ≥200 μm. Data are expressed as the mean (95% CI). Parameters are as defined in Table 2. ANOVA and corresponding pair-wise comparisons tests include only progressed eyes by disc and/or GPA, nonprogressed eyes, and healthy eyes. The ANOVA probability is in bold for comparisons with differences at $P \leq 0.05$.

* Significant difference (Tukey-Kramer HSD with $\alpha = 0.05$) between progressed and healthy eyes.

† Significant differences (Tukey-Kramer HSD with $\alpha = 0.05$) between nonprogressed and healthy eyes.

‡ Significant difference (Tukey-Kramer HSD with $\alpha = 0.05$) between progressed and healthy eyes and between progressed and nonprogressed eyes.